Guest-Induced Reversible Phase Transformation of Organic-Inorganic Phenylpiperazinium Antimony (III) Chlorides with Solvatochromic Photoluminescence

Xianli Li[a,†], *Chao Peng*[c,†], *Yonghong Xiao*[a], *Dongfeng Xue*[c,*], *Binbin Luo*[a,b,*], *and Xiao-Chun Huang*[a,b,*]

[a] *Department of Chemistry and Key Laboratory for Preparation and Application of Ordered Structural Materials of Guangdong Province, Shantou University, Shantou, Guangdong Province 515063, P. R. China*

[b] *Guangdong Laboratory of Chemistry and Fine Chemical Industry Jieyang Center, Jieyang, Guangdong Province 522000, P. R. China*

[c] *Multiscale Crystal Materials Research Center, Shenzhen Institute of Advanced Technology, Chinese Academy of Sciences, Shenzhen, Guangdong Province 518055, P. R. China*

Email: df.xue@siat.ac.cn; bbluo@stu.edu.cn; xchuang@stu.edu.cn

EXPERIMENTAL SECTION

Materials and methods

1-Phenylpiperazine (98%, Energy Chemical), antimony trichloride (99%, Alfa), HCl (37%, Guanghua Scientific), n-hexane (AR, Xilong Scientific), ethyl acetate (AR, Xilong Scientific), ethanol (AR, Xilong Scientific), methanol (AR, Xilong Scientific), acetone (AR, Xilong Scientific). All chemicals were used without further purification.

Synthesis of $(PhPi)_2SbCl_7 \cdot xH_2O$ single crystal

$(PhPi)_2SbCl_7 \cdot xH_2O$ single crystals were synthesized by mixing PhPi (0.2 mmol), $SbCl_3$ (0.1 mmol) and HCl (0.3 mL) into a 15 mL vessel equipped with a Teflon screw cap at 100 °C. After solids were totally dissolved, the precursors were cooled to room temperature to get block-like crystals.

Phase Transformation from $(PhPi)_2SbCl_7 \cdot xH_2O$ to $(PhPi)_2SbCl_7$-V

$(PhPi)_2SbCl_7 \cdot xH_2O$ block-like crystals were placed in a 50 mL Schlenk flask. After the vacuum treatment for 2 hours at room temperature, colorless microcrystals of $(PhPi)_2SbCl_7$-V were obtained.

Phase Transformation from $(PhPi)_2SbCl_7 \cdot xH_2O$ to $(PhPi)_2SbCl_7$-S

$(PhPi)_2SbCl_7$-S crystals were prepared by injecting 20 mL acetone (or methanol, ethanol, tetrahydrofuran, dioxane) into $(PhPi)_2SbCl_7$-V (0.1 g) for 1 day or refluxing $(PhPi)_2SbCl_7 \cdot xH_2O$ in acetone for 2 hours and placed overnight to get block-like microcrystals.

Synthesis of $(PhPi)Cl_2$

$(PhPi)Cl_2$ were obtained by adding HCl (2 mmol) into 1 mmol 1-phenylpiperazine in ethanol at 0 °C with vigorous stirring. The pale yellow solids of $(PhPi)Cl_2$ were precipitated by adding ethyl acetate.

Characterization

Single crystal X-ray diffraction (SC-XRD). SC-XRD tests were performed on Rigaku XtaLab Pro MM007HF DWX diffractometer at 298 K using Cu Kα radiation (λ= 1.5418 Å). The structures were solved by intrinsic phasing method using SHELXT[1] program implanted in Olex2[2]. Refinement with full matrix least squares techniques on F^2 was performed by using SHELXL[3]. Non-hydrogen atoms were anisotropically refined and all hydrogen atoms were generated based on riding mode.

Powder X-ray diffraction. PXRD patterns were recorded on MiniFlex 600 (Rigaku) to examine the crystalline phase

UV-vis absorption. UV-vis spectra were measured on Lambda 950 UV-vis Spectrometer

(PerkinElmer).

Photoluminescence (PL) spectra and excitation (PLE) spectra. Both of PL and PLE spectra were collected on PTI QM-TM (Photon Technology International).

Absolute PL QY. Absolute PL QY was recorded on a HAMAMATSU C11347 spectrometer with integrating sphere with the excitation wavelength of 340 nm for all samples.

Thermogravimetric analyses (TGA). TGA were performed on a SHMADZU TA-50 thermal analyzer with a heating rate of 10 °C min^{-1} from 30 to 700 °C under nitrogen gas flow

Photoluminescence lifetime. PL lifetime tests were collected on Edinburgh Instruments (FL 900). The PL decay curves are fitted with exponential function as given in the following expression:

$$I(t) = \sum_{n}^{i=1} A_i e^{-\frac{t}{\tau_i}}$$

where *I(t)* is the PL intensity at time *t*, *t* is the time, A_i represents the relative weights of the decay components at $t = 0$, τ_i denotes the decay time for the exponential components. The average lifetime is calculated based on the expression below:

$$\tau_{ave} = \sum_{n}^{i=1} A_i \tau_i^2 / \sum_{n}^{i=1} A_i \tau_i$$

Density function theory (DFT) calculation. Spin-polarized DFT calculations were conducted using the Vienna Ab-Initio Simulation Package (VASP).[4-5] The Perdew-Burke-Ernzerhof (PBE) functional within the Generalized Gradient Approximation (GGA) was applied to treat the exchange-correlation.[5-7] The projector-augmented wave (PAW) method was used to describe the core electrons.[8-9] The valence electronic states were expanded in plane-wave basis sets with a cutoff energy of 450 eV. The force convergence criterion was set to 0.03 eV/Å. The DFT-D3 method with Becke-Johnson (BJ) damping was used to describe the dispersion interactions.[10-11] During geometry optimization, all atoms were allowed to relax with the lattice constant being fixed. We used a k-mesh of (3×1×4) to optimize the structure of the $(PhPi)_2SbCl_7$-V and k-meshes of (2×1×4) and (4×4×2) for $(PhPi)_2SbCl_7 \cdot xH_2O$ and $(PhPi)_2SbCl_7$-S, respectively.

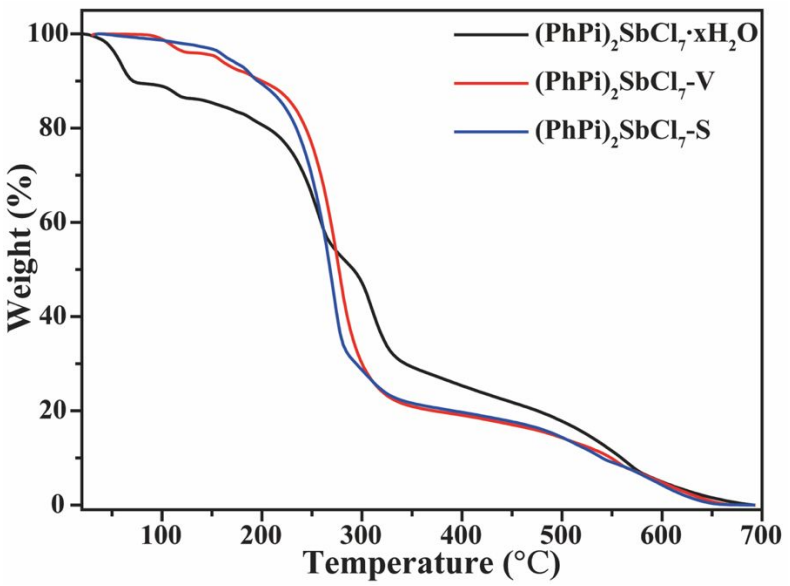

Figure S1. TGA of $(PhPi)_2SbCl_7 \cdot xH_2O$, $(PhPi)_2SbCl_7$-V and $(PhPi)_2SbCl_7$-S.

Table S1 Crystal data of $(PhPi)_2SbCl_7 \cdot xH_2O$, $(PhPi)_2SbCl_7$-V and $(PhPi)_2SbCl_7$-S

	$(PhPi)_2SbCl_7 \cdot xH_2O$	$(PhPi)_2SbCl_7$-V	$(PhPi)_2SbCl_7$-S
Empirical formula	$C_{20}H_{36}Cl_7N_4O_2Sb$	$C_{20}H_{32}Cl_7N_4Sb$	$C_{20}H_{32}Cl_7N_4Sb$
Formula weight	734.43	698.39	698.39
Temperature/K	298.86(10)	298.3(7)	298(2)
Radiation	Cu *K*α (λ = 1.54184 Å)	Cu *K*α (λ = 1.54184 Å)	Cu *K*α (λ = 1.54184 Å)
Crystal system	monoclinic	monoclinic	triclinic
Space group	*C*2/*c*	*C*2/*c*	$P\bar{1}$
a/Å	15.8872(3)	12.74300(10)	10.2371(3)
b/Å	27.0504(5)	28.0958(3)	10.6199(3)
c/Å	8.1864(2)	8.45780(10)	15.4570(3)
α/°	90	90	99.953(2)
β/°	101.837(2)	103.0480(10)	102.546(2)
γ/°	90	90	114.672(3)
V/Å^3	3443.33(13)	2949.92(5)	1423.28(7)
Z	4	4	2
ρ_{calc} (g/cm^3)	1.417	1.573	1.630
completeness to θ_{max}	97%	100%	99%
GOF	1.089	1.257	1.095
R_{int}	0.0352	0.0173	0.0376
final *R* indexes [$I > 2\sigma(I)$][a]	R_1 =0.0294, wR_2 = 0.0827	R_1 =0.0644, wR_2 = 0.1766	R_1 = 0.0444, wR_2 = 0.1228
R indexes (all data)[a]	R_1 = 0.0311, wR_2 = 0.0835	R_1 = 0.0655, wR_2 = 0.1770	R_1 = 0.0488, wR_2 = 0.1255
largest diff. peak and hole, e Å^{-3}	0.52/-0.63	0.94/-0.79	1.67/-1.10

[a] $R_1 = \Sigma||F_o|-|F_c||/\Sigma|F_o|$; $wR_2 = \{[\Sigma w(F_o^2-F_c^2)^2]/\Sigma[w(F_o^2)^2]\}^{1/2}$; $w = 1/[\sigma^2(F_o^2)+(aP)^2+bP]$, where $P = [\max(F_o^2, 0) + 2Fc^2]/3$ for all data.

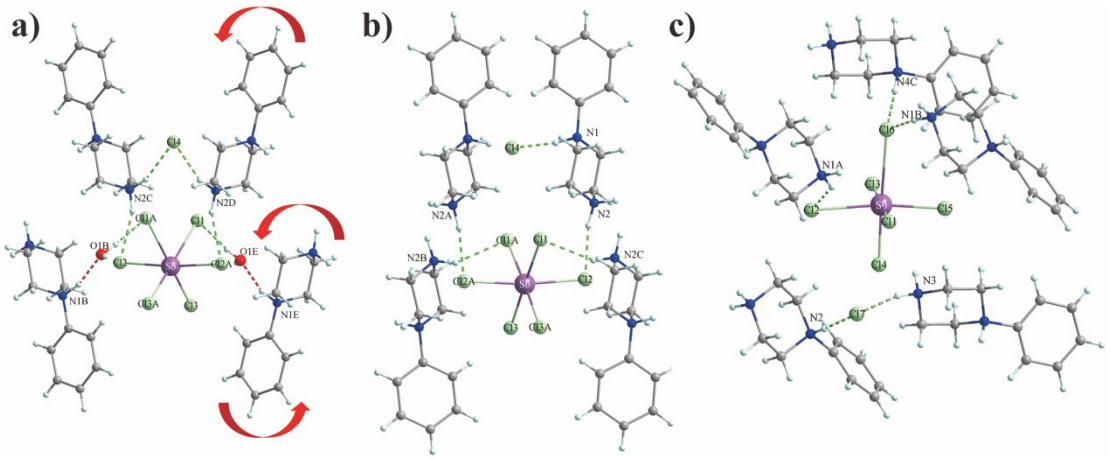

Figure S2. Hydrogen bonding interaction (denoted by dash line) in (a) $(PhPi)_2SbCl_7 \cdot xH_2O$, (b) $(PhPi)_2SbCl_7$-V and (c) $(PhPi)_2SbCl_7$-S. The arrows in (a) denote the rotary direction of PhPi cations after phase transformation from $(PhPi)_2SbCl_7 \cdot xH_2O$ to $(PhPi)_2SbCl_7$-V.

As for $(PhPi)_2SbCl_7 \cdot xH_2O$, the occupancy of $PhPi^{2+}$, Cl1, Cl2 and Cl3 is 1.0, while that of Sb1 and Cl4 is 0.5 in the asymmetric unit. The similar occupancy is happened in $(PhPi)_2SbCl_7$-V, except for the disordered Cl4. For this free Cl in $(PhPi)_2SbCl_7$-V, Cl4 and Cl4A contribute the occupancy of 0.5 in total. The occupancy of all atoms in the asymmetric unit is 1.0 in $(PhPi)_2SbCl_7$-S. The disordered Cl5 and Cl5A contribute occupancy of 1.0 in total.

Table S2. Bond length of $(PhPi)_2SbCl_7 \cdot xH_2O$

Bond	Length (Å)
Sb-Cl1	2.907(1)
Sb-Cl2	2.683(1)
Sb-Cl3	2.448(1)
Sb-Cl1A	2.907(1)
Sb-Cl2A	2.683(1)
Sb-Cl3A	2.448(1)
Standard deviation	0.187

A: 1-X, +Y, -0.5-Z

Table S3. Bond length of $(PhPi)_2SbCl_7$-V

Bond	Length (Å)
Sb-Cl1	2.833(3)
Sb-Cl2	2.665(3)
Sb-Cl3	2.501(3)
Sb-Cl1A	2.833(3)
Sb-Cl2A	2.665(3)
Sb-Cl3A	2.501(3)
Standard deviation	0.136

A: 1-X, +Y, 1.5-Z

Table S4. Bond length of $(PhPi)_2SbCl_7$-S

Bond	Length (Å)
Sb-Cl1	2.799(2)
Sb-Cl2	2.788(2)
Sb-Cl3	2.511(2)
Sb-Cl4	2.420(2)
Sb-Cl5A	2.575(8)
Sb-Cl5	2.526(2)
Sb-Cl6	3.143(1)
Standard deviation	0.244

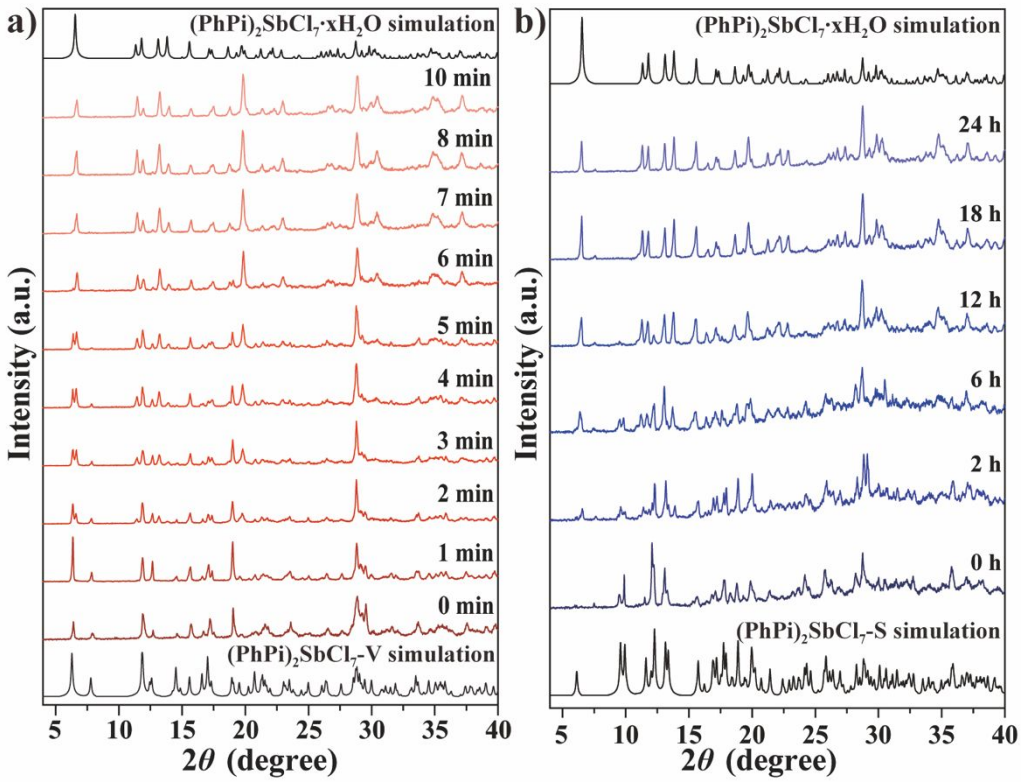

Figure S3. PXRD of (a) $(PhPi)_2SbCl_7$-V and (b) $(PhPi)_2SbCl_7$-S powders by placing in open air at different time.

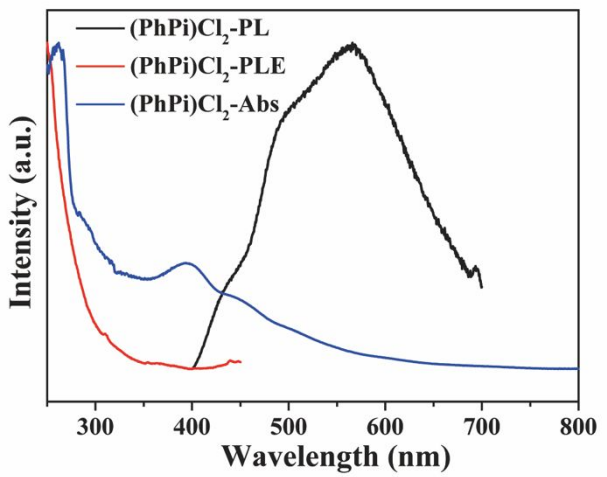

Figure S4. Absorption, PL and PLE spectra of $(PhPi)Cl_2$.

Table S5. PL lifetime of $(PhPi)_2SbCl_7$-V

τ_1	A_1	τ_2	A_2	τ_{avg}
0.135 μs	96.2 %	1.51 μs	3.8 %	0.562 μs

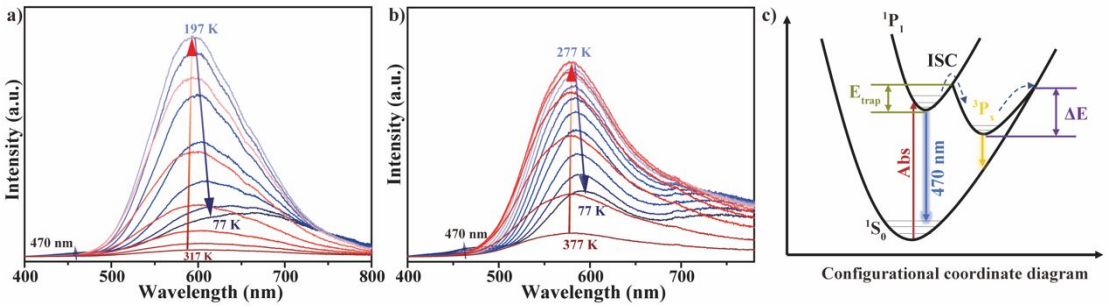

Figure S5. Temperature-dependent PL of $(PhPi)_2SbCl_7$-V (a) and $(PhPi)_2SbCl_7$-S (b), 355 nm is used as the excitation wavelength. (c) Configurational coordinate diagram showing the thermal activation energy and energy barrier of phonon-assisted nonradiative recombination.

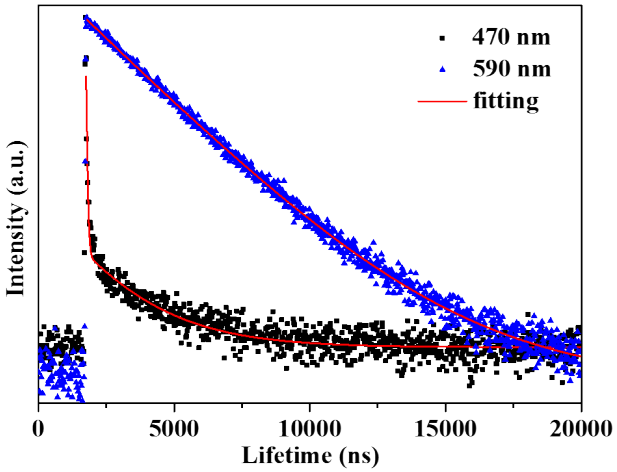

Figure S6. TRPL of $(PhPi)_2SbCl_7$-V at 77 K. 355 nm is used as the excitation wavelength.

Table S6. Fitting results of PL decay at 470 nm for $(PhPi)_2SbCl_7$-V at 77 K

τ_1	A_1	τ_2	A_2	τ_{avg}
0.040 μs	92.4%	2.322 μs	7.6%	1.931 μs

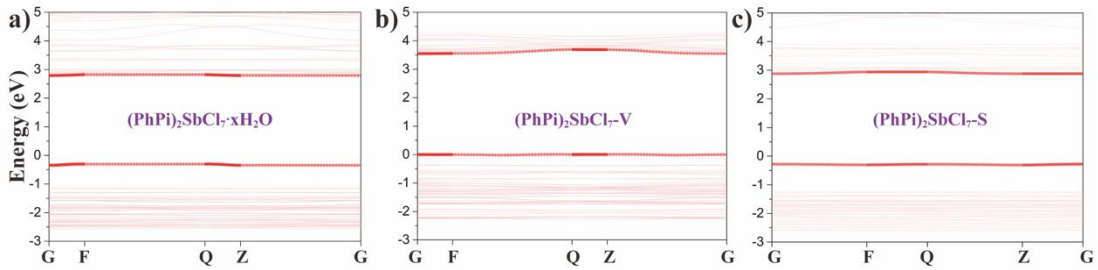

Figure S7. The band structures of $(PhPi)_2SbCl_7 \cdot xH_2O$ (a), $(PhPi)_2SbCl_7$-V (b) and $(PhPi)_2SbCl_7$-S (c), respectively.

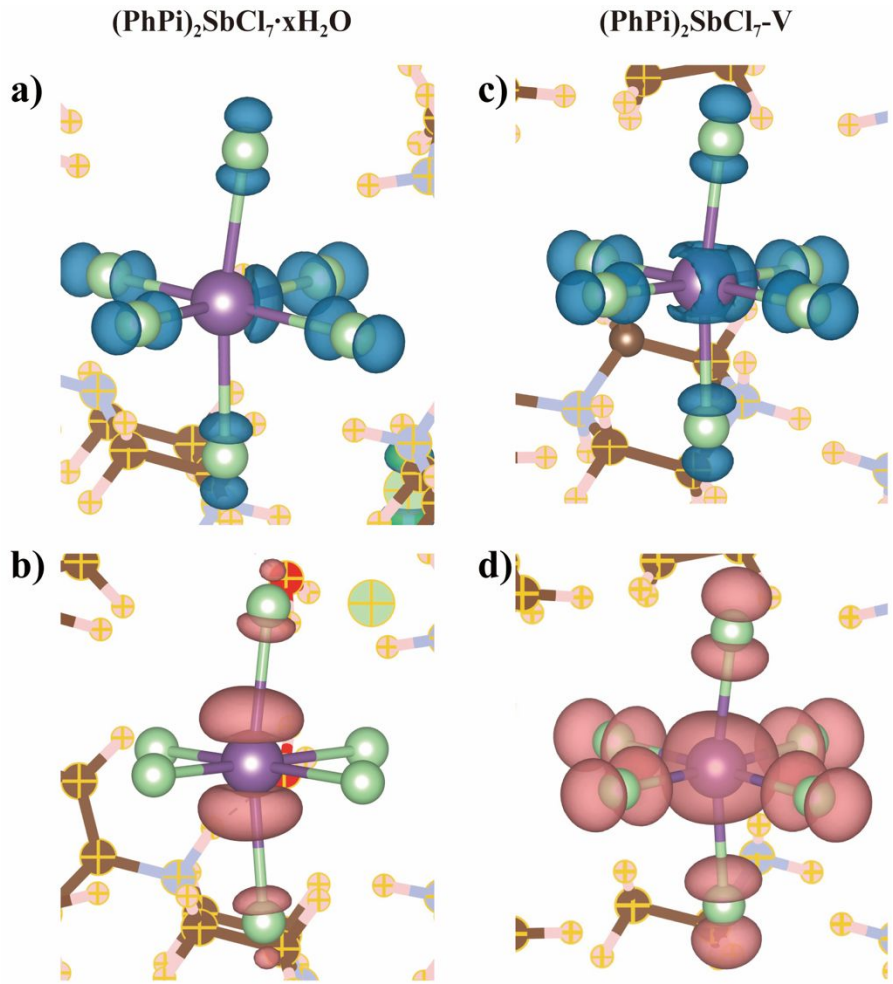

Figure S8. The charge density contours of the photogenerated hole (a, c) and the photogenerated electron (b, d) in $(PhPi)_2SbCl_7 \cdot xH_2O$ and $(PhPi)_2SbCl_7$-V

REFERENCE:

1. Sheldrick, G. M., SHELXT-Integrated Space-Group and Crystal-Structure Determination. *Acta Cryst. A* **2015**, *71*, 3-8.
2. Dolomanov, O. V.; Bourhis, L. J.; Gildea, R. J.; Howard, J. A. K.; Puschmann, H., OLEX2: A Complete Structure Solution, Refinement and Analysis Program. *J. Appl. Crystallogr.* **2009**, *42* (2), 339-341.
3. Sheldrick, G. M., A Short History of SHELX. *Acta Cryst. A* **2008**, *64*, 112-122.
4. Kresse, G.; Furthmüller, J., Efficient Iterative Schemes for *ab-Initio* Total-Energy Calculations Using a Plane-Wave Basis set. *Phys. Rev. B* **1996,** *54* (16), 11169-11186.
5. Kresse, G.; Furthmüller, J., Efficiency of *ab-Initio* Total Energy Calculations for Metals and Semiconductors Using a Plane-Wave Basis Set. *Comput. Mater. Sci.* **1996,** *6* (1), 15-50.
6. Perdew, J. P.; Burke, K.; Ernzerhof, M., Generalized Gradient Approximation Made Simple. *Phys. Rev. Lett.* **1996,** *77* (18), 3865-3868.
7. Kresse, G.; Hafner, J., *Ab Initio* Molecular-Dynamics Simulation of the Liquid-Metal–Amorphous-Semiconductor Transition in Germanium. *Phys. Rev. B* **1994,** *49* (20), 14251-14269.
8. Kresse, G.; Joubert, D., From Ultrasoft Pseudopotentials to the Projector Augmented-Wave Method. *Phys. Rev. B* **1999,** *59* (3), 1758-1775.
9. Blöchl, P. E.; Jepsen, O.; Andersen, O. K., Improved Tetrahedron Method for Brillouin-Zone Integrations. *Phys. Rev. B* **1994,** *49* (23), 16223-16233.
10. Grimme, S.; Ehrlich, S.; Goerigk, L., Effect of the Damping Function in Dispersion Corrected Density Functional Theory. *J. Comput. Chem.* **2011,** *32* (7), 1456-1465.
11. Grimme, S.; Antony, J.; Ehrlich, S.; Krieg, H., A Consistent and Accurate *ab Initio* Parametrization of Density Functional Dispersion Correction (DFT-D) for the 94 Elements H-Pu. *J. Chem. Phys.* **2010,** *132* (15), 154104.